Available online at www.sciencedirect.com

SciVerse ScienceDirect

Ceramics International 38 (2012) 5393–5399

CERAMICS INTERNATIONAL

www.elsevier.com/locate/ceramint

The effects of nanoparticle addition on the densification and properties of SiC

Valmikanathan P. Onbattuvelli [a], Ravi K. Enneti [b,*], Sundar V. Atre [a]

[a] Oregon State University, Corvallis, OR, USA
[b] Global Tungsten Powders, Towanda, PA, USA

Received 24 February 2012; received in revised form 19 March 2012; accepted 20 March 2012
Available online 28 March 2012

Abstract

The effects of nanoparticle addition on the pressureless sintering of injection molded and thermally debound silicon carbide (SiC) samples were studied. The influence of increased powder content and reduced particle size on the densification, microstructure and properties are discussed. The sintered parts of bimodal μ–n SiC mixtures exhibited comparable sintered density but lower shrinkage than the corresponding monomodal μ-SiC powder mixtures. Additionally, the mechanical and thermal properties of sintered monomodal and bimodal SiC samples were measured and compared with literature data for conventional monomodal μ-SiC systems.

Keywords: A. Sintering; C. Hardness; C. Thermal conductivity; Nanoparticle; Silicon carbide; Toughness; Thermal diffusivity

1. Introduction

The development of methods to improve the densification and the ensuing thermal and mechanical properties has been a crucial issue in the processing of silicon carbide (SiC) [1–5]. Mass transport during sintering depends upon surface (ε_s) and grain boundary energies (ε_b) [6,7]. For example, the ratio $\varepsilon_b/\varepsilon_s$ for SiC is ~0.97 due to the presence of covalent bonds [8]. As $\varepsilon_b/\varepsilon_s$ approaches unity, achieving full densification becomes difficult. Consequently, several alternative techniques have been developed to improve the SiC densification. A well-explored method is the addition of densification additives (aids) that allow liquid phase sintering [1–5,9–12] of SiC. Solid solubility in the eutectic liquid improves transport rates responsible for grain coarsening and densification [13,14].

Prior reports investigated SiC densification by exploring material and process parameters. As mentioned earlier, the self-diffusion of SiC is extremely slow and requires various additives to assist sintering [15]. For example, Prochazka demonstrated that B and C could be used as solid-state sintering aids for SiC [16]. She and Ueno studied the effect of varying the amount of Al_2O_3–Y_2O_3 on the porosity [9]. Similarly, Sciti and Bellosi compared the combinations of Al_2O_3–Y_2O_3 and La_2O_3–Y_2O_3, as sintering aids for SiC densification [3]. Conventionally, SiC is densified by pressure-assisted sintering including hot pressing [17] and more recently plasma pressure compaction [18]. In contrast, pressureless sintering is important in the context of powder injection molding (PIM) of complex shapes. The effects of sintering temperature and hold time on the pressureless sintering have been extensively studied in the past. For example, She and Ueno [9] and Jin et al. [19] reported the increase in the sintered density of SiC with the increase in the sintering temperature. On the other hand, Izhevskyi et al. [11] and Rodriguez et al. [20] noticed an increase in the sintered density with higher hold time at the sintering temperature. A detailed literature review on such prior work on SiC densification is reported elsewhere [21].

Our recent research work successfully demonstrated an increase in powder packing density with the addition of nanoparticles (n) to submicron (μ) particles, forming bimodal μ–n powder mixtures [22,23]. For example, the powder content is found to increase from 53 to 65 vol.% when SiC nanoparticles are added to the monomodal submicron (μ) sized SiC powders. The implication of such nanoparticle addition is discussed in the past in the context of thermal and

* Corresponding author.
E-mail addresses: ravi.enneti@globaltungsten.com (R.K. Enneti), sundar.atre@oregonstate.edu (S.V. Atre).

0272-8842/$36.00
http://dx.doi.org/10.1016/j.ceramint.2012.03.049

rheological properties of the powder–polymer mixtures, mold filling behavior and polymer removal kinetics of the injection molded bimodal μ–n SiC samples [22,24]. In a similar manner, the effect of nanoparticle addition on the sintering of SiC at different time–temperature combinations is the focus of the current work. Further, the sintered density, shrinkage, mechanical and thermal properties of the sintered bimodal μ–n samples are compared with that of monomodal μ-SiC samples processed under identical conditions.

2. Experimental

2.1. Materials

The starting powder materials contain as-received., commercially available SiC (0.7 μm and 50 nm) with 5 wt.% AlN (20 nm) and 5 wt.% Y_2O_3 (50 nm) as the sintering additives. Powder injection molded bimodal μ–n SiC and monomodal μ-SiC samples were solvent and thermally debound prior to sintering. The molding and debinding conditions used are detailed elsewhere [20,24]. Thermally debound bimodal (initial density of 1.9 g/cc, 65% relative density) and monomodal (initial density of 1.67 g/cc, 51% relative density) SiC samples were pre sintered at 1500 °C for 2 h and sintered at temperatures between 1800 and 2000 °C for two different hold times of 2 and 4 h under argon atmosphere. The sintering conditions were selected based on the literature review on SiC densification as presented in Fig. 1 [1–3,9–11,25–29]. The density for all the sintered samples was measured with a lab-built Archimedes density apparatus. Microstructural analysis was conducted on the surfaces of thermally debound SiC samples using a Quanta^{TM}–FEG (FEI) dual beam scanning electron microscope (SEM) coupled with an energy dispersive X-ray spectrometer (EDS). SEM images of each sample were collected in two different magnifications for better comparison. The thermal diffusivity of the samples was measured with a LFA-457 (Netzsch) laser flash apparatus. TA Instruments-Q-500 was used to measure the specific heat (C_p) of the sintered samples. Vickers hardness and indentation toughness of the sintered SiC samples were measured using a Leco microhardness tester.

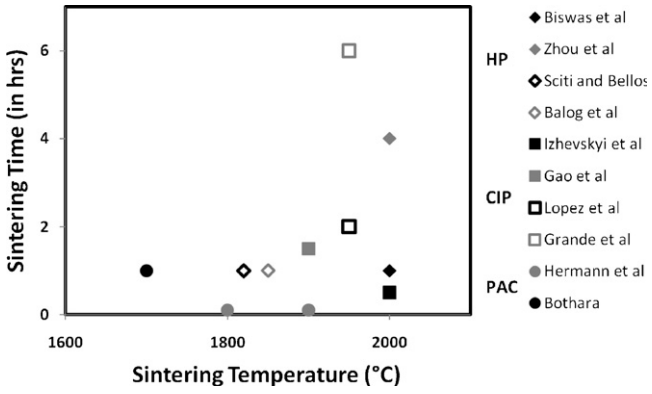

Fig. 1. Processing window for sintering conditions for SiC based on the literature reports.

3. Results and discussion

Being classified as difficult to sinter ceramic, the densification of SiC was promoted by liquid phase sintering, accompanying solution-reprecipitated SiC grains and an intergranular glassy phase [4]. Combination of AlN and Y_2O_3 is one of the most commonly reported sintering additives for SiC and is thus used in the current study [1,29–32]. During sintering, Y_2O_3 reacts with the surface oxides from AlN and SiC and forms a rare earth alumino-silicate glass melt. With the dissolution of the small SiC particles, the resulting liquid could be regarded as Y–Si–Al–O–C glass melt. On cooling, the Y–Si–Al–O–C constitute the intergranular phases in the SiC ceramics. The liquid phase formation is accompanied by the elimination of pores which is followed by shrinkage/densification.

From the densification plots presented in Fig. 2, it can be seen that the densification of both monomodal and bimodal SiC is initiated below 1800 °C. SEM studies (Figs. 3 and 4) on these samples confirmed a liquid phase formation at ~1500 °C, which is much lower than the previously reported values for monomodal μ-SiC samples as listed in Table 1 [2,3,9,33–35]. The reduction in the liquid phase formation temperature for both monomodal and bimodal SiC in the current study can be attributed to the inclusion of n-Y_2O_3 as sintering additive. The increased surface area of the nanosized additive in turn may have increased the reaction rate between Al_2O_3, Y_2O_3 and surface SiO_2 shifting the eutectic formation to relatively lower temperatures. Further sintering studies comparing bimodal SiC mixtures to those containing μ-sized additives are required to understand the effect of SiC and Y_2O_3 nanoparticles addition on the liquid phase formation. Additionally, a novel nanorod formation is noticed with the monomodal SiC at 1550 °C (Fig. 4d). This has not been previously reported in the literature. The reason for the presence of nanorods and their absence in bimodal SiC is not clear at this stage of research. Future experiments including as series of XRD analysis on the thermally debound SiC samples may explain the above mentioned behavior.

Even though the liquid phase is formed at relatively lower temperatures, densification above 90% is exhibited by both monomodal and bimodal SiC only at temperatures greater than 1900 °C. This may be attributed to the slower solution–

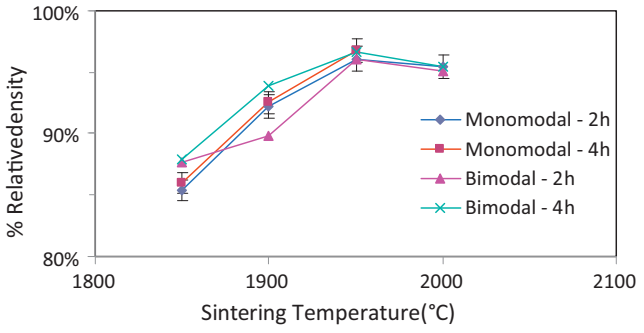

Fig. 2. Effect of sintering temperature on the densification of monomodal and bimodal SiC.

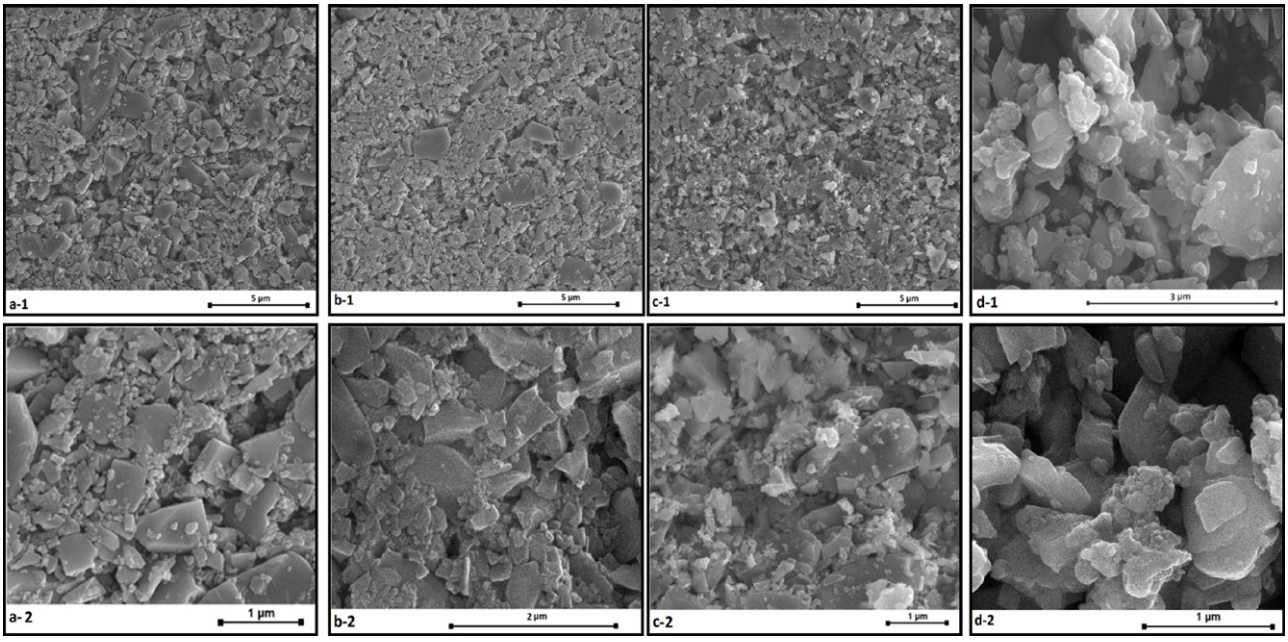

Fig. 3. SEM images revealing the transition of bimodal SiC samples from thermally debound stage to the onset of liquid phase formation, (a) 500 °C, (b) 1100 °C, (c) 1300 °C and (d) 1550 °C.

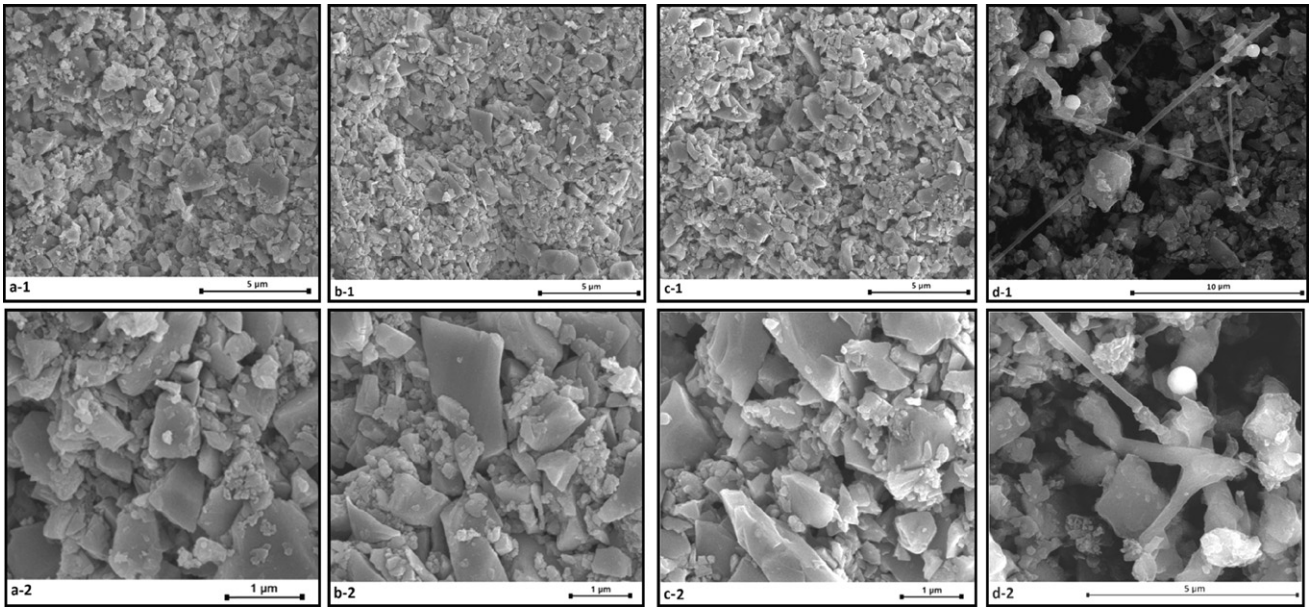

Fig. 4. SEM images revealing the transition of monomodal SiC samples from thermally debound stage to the onset of liquid phase formation, (a) 500 °C, (b) 1100 °C, (c) 1300 °C and (d) 1550 °C.

Table 1
Literature review on the liquid phase formation temperature for SiC densification.

Refs. #	Author	Initial SiC particle size (μm)	Type of sintering additive	Liquid phase formation temperature
[2]	Grande et al.	$\alpha - 0.6$	4.72% Al_2O_3–2.73% Y_2O_3	1820 °C
[3]	Sciti and Bellosi	–	6%Al_2O_3–4%Y_2O_3	1710 °C
[33]	Lee et al.	$\beta - 0.27$	5.3% Y_2O_3–4.7%Al_2O_3	1800 °C
[34]	Can et al.	–	5% Y_2O_3–5%Al_2O_3	1600 °C
[35]	Guo et al.	$\alpha - 0.75$	6.25% Al_2O_3–3.75% Y_2O_3	1760 °C
[36]	He et al.	$\beta - 0.8$	6% MgO–1% Al_2O_3–1% Y_2O_3	
[9]	She and Ueno	$\alpha - 0.6$	6.25% Al_2O_3–3.75% Y_2O_3	

Table 2
Prior reports on additive-assisted pressureless sintering of SiC.

Refs. #	Author	SiC particle size (μm)	Sintering aid		Net shaping and densification (with pressure in MPa)	Sintering conditions			% Relative density
			Nature	% Content		Atm.	Temp. (°C)	Hold time (h)	
[5]	Ortiz et al.	–	Al_2O_3–Y_2O_3	14.92–11.22	UP (50) + CIP (350)	Ar	1950	1	98%
[9]	She and Ueno	$\alpha - 0.6$	Al_2O_3–Y_2O_3	6.25–3.75	UP (3) + CIP (200)	Ar	2000	1	98%
[26]	Gao et al.	–	Al_2O_3–Y_2O_3	5–5	UP (25) + CIP (200)	N_2	1900	1.5	98%
[35]	Guo et al.	$\alpha - 0.75$	Al_2O_3–Y_2O_3	6.25–3.75	UP (100) + CIP (250)	Vac.	1860	0.75	96.1%
[37]	Pujar et al.	–	Al_2O_3–Y_2O_3	12.5–7.5	UP (50) + CIP (350)	Ar	1900	0.5	96%
[38]	Magnani et al.	$\beta - 0.72$	Al_2O_3–Y_2O_3	6–4	UP (67) + CIP (250)	Ar	1875	0.5	97.1%
[39]	Suzuki and Sasaki	–	Al_2O_3	15	UP (20) + CIP (200)	N_2	1950	5	97%
[20]	Rodriguez et al.	–	Al_2O_3–Y_2O_3	5–5	UP	Ar	1950	1	98.8%
								3	97.3%
								5	96.7%
								7	94.9%
[40]	Zhang et al.	$\alpha - 0.5$	Al_2O_3–Y_2O_3	4.5–4.5	–	N_2	1950	1	98%

reprecipitation of SiC from the Y–Si–Al–O–C glass melt. Additionally, varying the hold time is found to have little effect on the SiC densification for the range of times (2–4 h) that was investigated. Bimodal SiC sintered at 1950 °C showed 97% densification which is comparable to that of monomodal SiC (96%). A comparative list of presented in the Table 2 confirms the proximity of findings from the present study on sintered density to previously reported values [5,9,20,26,35,37–40].

In addition to above densification trends, a decrease in density is noticed after ~1950 °C. This in turn can be correlated with the weight loss of up to 11% and 13% experienced by monomodal and bimodal SiC samples during sintering as shown in Fig. 5. Previous reports explained this behavior as the outcomes of the following reactions that occur at temperatures ≥1800 °C [35,39].

$$SiC_{(s)} + Al_2O_{3(s)} \rightarrow SiO_{(g)}\uparrow + Al_2O_{(g)}\uparrow + CO_{(g)}\uparrow$$
$$SiC_{(s)} + 2Y_2O_{3(s)} \rightarrow SiO_{(g)}\uparrow + 4YO_{(g)}\uparrow + CO_{(g)}\uparrow$$

As shown in the above equations, excess sintering additives present in the powder mixture reacts with SiC to form volatile monoxides of Al and Y along with CO. This material loss opens up new pores at sintering temperatures leading to reduction in the % density. From Fig. 5 it can be seen that the bimodal SiC samples experience more weight loss than the monomodal samples at any given sintering temperature–time conditions. This could be due to the increased reactivity by the high surface area n-SiC present in the bimodal mixtures. Similar results on weight loss has been reported qualitatively in the past by She and Ueno [9], Grande et al. [2], Guo et al. [35], Suzuki and Sasaki [39] arguing the necessity to optimize the sintering additive content prior to SiC sintering. Sintering techniques including plasma pressure compaction and microwave sintering have been suggested in the past to combat the above issues [29]. Additionally, the reason for weight loss at temperatures between 1000 and 1800 °C is not clear at this stage of research. Future experiments including TGA-assisted–mass spectroscopy and are required to comparatively analyze the effect of n-SiC inclusion on the weight loss in the bimodal SiC samples.

As mentioned earlier, higher initial powder packing density (solids loading – Φ) is important for improving the sintered density and ensuing properties. Such higher green density in turn corresponds to lesser % shrinkage and thus more dimensional control. As shown in Fig. 6, an isometric shrinkage of up to 15% is noticed in bimodal μ–n SiC samples confirming the dimensional precision. The plot is also extended to compare ~20% shrinkage noticed in the monomodal μ-SiC samples

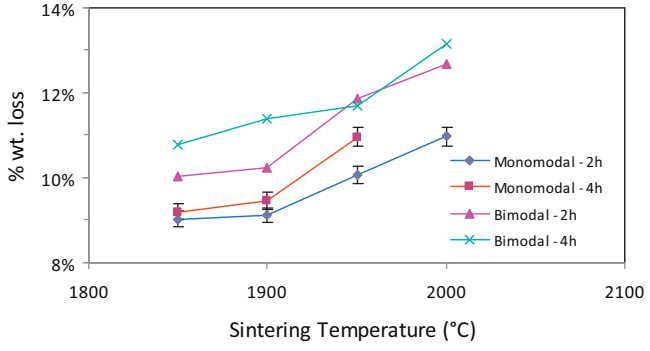

Fig. 5. Weight loss experienced by monomodal and bimodal SiC as a function of sintering temperature.

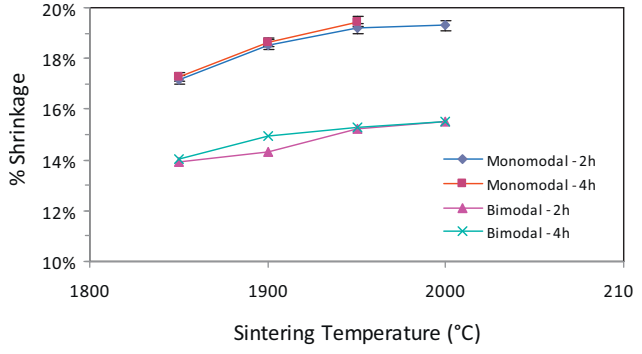

Fig. 6. Isometric shrinkage of monomodal and bimodal SiC as a function of sintering temperature.

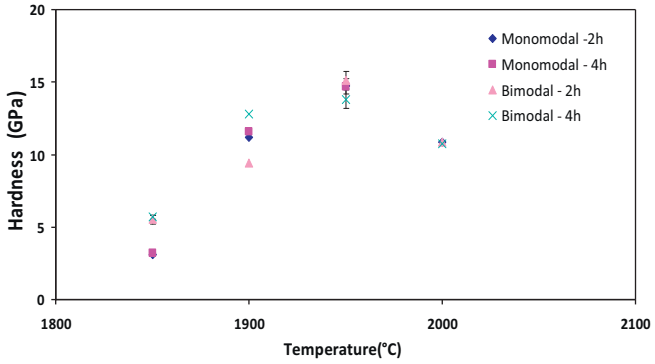

Fig. 7. Vickers hardness of monomodal and bimodal SiC as a function of sintering temperature.

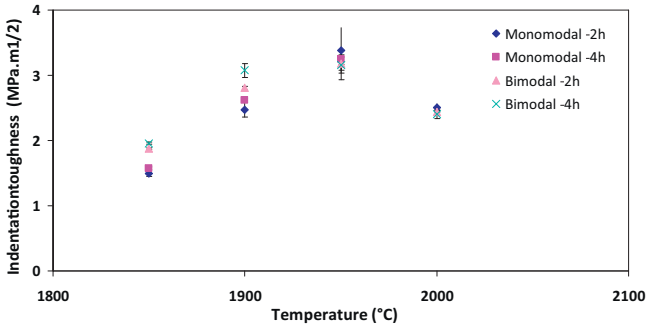

Fig. 8. Indentation toughness of monomodal and bimodal SiC as a function of sintering temperatures.

under similar sintering conditions (Fig. 6). Similar shrinkage value of 19% is reported in the past by Klemens et al. for the extruded monomodal μ-SiC powder mixtures [41]. This comparison confirms the novelty of bimodal μ–n powder mixtures where higher densification is achieved yet with relatively lower shrinkage. Thus, in addition to the increased sintered densities, using bimodal μ–n SiC powder mixtures exhibited a significant lowering in the shrinkage as shown in Fig. 6. The lower shrinkage observed for bimodal samples can be directly attributed to a higher solids loading relative to the monomodal samples.

Fig. 7 plots the Vickers hardness values obtained for bimodal and monomodal SiC samples sintered at different temperatures–time combinations. The hardness of SiC depends on factors such as sintered density, grain size and amount of secondary glassy phase. The Vickers hardness of both monomodal and bimodal SiC increased with increase in sintering temperature due to the corresponding densification process. A maximum hardness of 14.7 GPa and 15.1 GPa was exhibited by monomodal and bimodal SiC samples sintered at 1950 °C for 4 h, respectively. These values are comparatively lesser than the earlier reported measurements for monomodal SiC samples as listed in Table 3 [3,5,9,29,30,35,38–40]. This could be due to incomplete densification as well as the increase in the weight loss of the SiC samples with the sintering temperatures as discussed earlier. Further, grain growth due to expedited liquid phase formation could also be a reason for such reduced hardness values. For example, prior reports by Sciti and Bellosi (hot pressing of monomodal μ-SiC) [3] and Bothara et al. (plasma pressure compaction of monomodal n-SiC) [29] reported hardness values ≥20 GPa, with greater densification achieved at lower temperatures. Their work suggests the necessity for an external source (pressure, electric field) to achieve densification yet with suppressed grain growth. She and Ueno [9], on the other hand discussed the detrimental effect of excessive sintering additives on the properties, arguing the necessity to optimize the additives content prior to SiC sintering. The measured indentation toughness of the monomodal and bimodal (Fig. 8) SiC showed a similar trend to that of the hardness values. This is due its exhibition of a density–microstructure–property relationship similar to that of hardness values. A maximum indentation toughness of 3.4 MPa $m^{1/2}$ and 3.2 MPa $m^{1/2}$ is noticed for monomodal and bimodal SiC samples sintered at 1950 °C for 4 h, respectively. Such lower toughness values compared to previous reports (Table 3) could be due to the combined effect of weight loss and grain growth. Fig. 9 plots the thermal diffusivity values obtained for monomodal and bimodal samples sintered at different temperatures. The diffusivity values were expected to be equal for monomodal and bimodal SiC samples as they show similar densification trends. However, the thermal diffusivity of bimodal samples (~35 mm^2/s) sintered at 1950 °C were found to be higher than that of monomodal samples (~30 mm^2/s) by

Table 3
Prior reports on the mechanical properties of monomodal SiC.

Refs. #	Author	Sintering aid		Sintering conditions			% Relative density	Toughness (MPa $m^{1/2}$)	Hardness (GPa)
		Nature	% Content	Atm.	Temp. (°C)	Hold time (h)			
[3]	Sciti and Bellosi	Al_2O_3–Y_2O_3	6–4	–	1780	0.5	98%	3.1	22
[5]	Ortiz et al.	Al_2O_3–Y_2O_3	14.92–11.22	Ar	1950	1	98%	3.3	17.3
[9]	She and Ueno	Al_2O_3–Y_2O_3	6.25–3.75	Ar	1900	1	98%	7.5	19.5
					1950		97.5%	6.5	18
					2000		97%	6	17
[29]	Manish Bothara	AlN–Y_2O_3	5–5	Ar	1700	1	99.6%	5	20
[30]	Nader et al.	AlN–Y_2O_3	2.95–10.34	N_2	1925	14	–	2.8	–
[35]	Guo et al.	Al_2O_3–Y_2O_3	6.25–3.75	Vaccum.	1860	0.75	96.1%	5.2	20
[38]	Magnani et al.	Al_2O_3–Y_2O_3	6–4	Ar	1875	0.5	97.1%	4.5	21
[39]	Suzuki and Sasaki	Al_2O_3	15	N_2	1950	5	97%	4.3	21.9
[40]	Zhang et al.	Al_2O_3–Y_2O_3	4.5–4.5	N_2	1950	1	98%	2	–

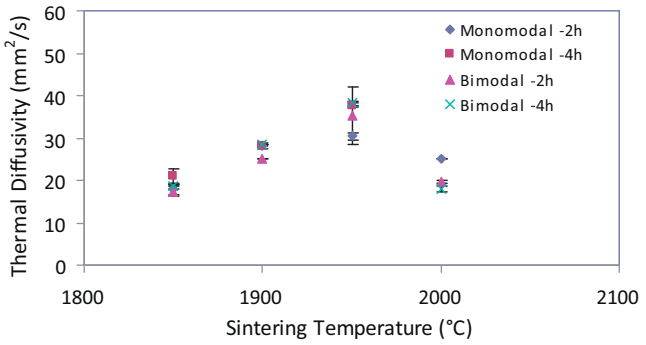

Fig. 9. Thermal diffusivity of monomodal and bimodal SiC as a function of sintering temperatures.

5 mm^2/s. Despite the higher weight loss experienced by bimodal samples, such a rise in the thermal diffusivity values strengthens our earlier proposal of grain growth due to expedited liquid phase formation in the bimodal samples.

The C_p values for monomodal and bimodal SiC samples at different sintering temperatures are shown in Fig. 10. A nearly constant C_p value of 0.6 J/g K for monomodal and bimodal SiC samples is observed regardless of the sintering conditions. A similar C_p value of 0.65 J/g K is reported in the past by Zhou et al. for monomodal SiC system [12]. The thermal conductivity (K) is a product of thermal diffusivity, sintered density and C_p. Thus, factors such as sintered density, weight loss, grain growth and amount of intergranular glassy phase were found to affect

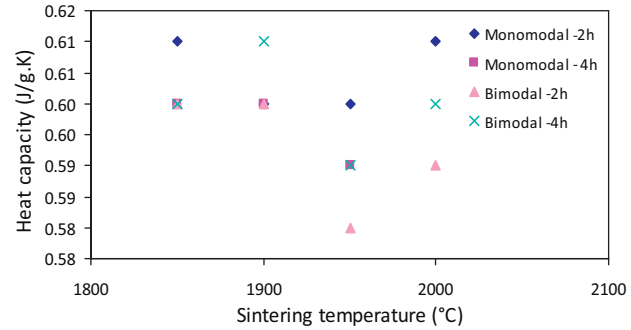

Fig. 10. C_p of monomodal and bimodal SiC as a function of sintering temperatures.

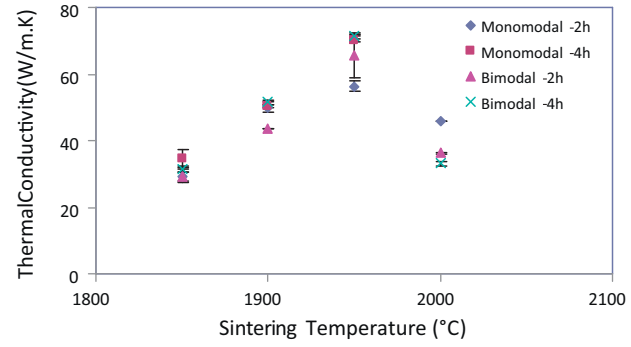

Fig. 11. Thermal conductivity of monomodal and bimodal SiC as a function of sintering temperatures.

the thermal conductivity of the given samples. These factors can explain the trends noticed in that thermal conductivity plots (Fig. 11) similar to that of the earlier discussed thermal diffusivity values. A maximum thermal conductivity of 73 W/m K was exhibited by bimodal SiC samples sintered at 1950 °C compared to that of 68 W/m K by the monomodal samples.

4. Conclusions

Bimodal μ–n and monomodal μ-SiC samples with the addition of nanosized Y_2O_3 as a sintering aid exhibited a liquid phase formation at lower temperatures than reported literature values for the pressureless sintering of SiC. The combined effect of increased powder content and reduced average particle size by nanoparticle addition are proposed as the reasons for 97% densification with only 14% shrinkage noticed in the bimodal SiC samples. A reduction noticed in the mechanical properties with an increase in the sintering temperature was attributed to the weight loss experienced by bimodal SiC samples. Higher thermal diffusivity and thermal conductivity values of bimodal SiC samples are suggested as the outcomes of higher densification and possible expedited grain growth despite the higher weight loss.

References

[1] K. Biswas, J. Schneider, G. Rixecker, F. Aldinger, Comparative bending creep behaviour of silicon carbide sintered with oxynitride additives, Scr. Mater. 53 (2005) 591–596.
[2] T.H. Grande, H. Sommerset, E. Hagen, K. Wiik, M.A. Einarsrud, Effect of weight loss on liquid-phase-sintered silicon carbide, J. Am. Ceram. Soc. 80 (4) (1997) 1047–1052.
[3] D. Sciti, D.A. Bellosi, Effects of additives on densification, microstructure and properties of liquid-phase sintered silicon carbide, J. Mater. Sci. 35 (2000) 3849–3855.
[4] Y. Lee, Y.W. Kim, M. Mitomo, Fabrication of dense nanostructured silicon carbide ceramics through two-step sintering, J. Am. Ceram. Soc. 86 (10) (2003) 1803–1805.
[5] A.L. Ortiz, A.M. Bernabe, O.B. Lopez, A.D. Rodrıguez, F. Guiberteau, N.P. Padture, Effect of sintering atmosphere on the mechanical properties of liquid-phase-sintered SiC, J. Eur. Ceram. Soc. 24 (2004) 3245–3249.
[6] R.M. German, Sintering Theory and Practice, John Wiley and Sons, Inc., NY, USA, 1996.
[7] Y. Inomata, in: S. Somiay (Ed.), Proceeding of International Symposium on Ceramic Components for Engine, KTK Scientific Publishers, Tokyo, 1984, , 253 pp.
[8] Y. Uemura, Y. Inomata, Z. Inoue, A grain boundary of α-SiC bicrystals, J. Mater. Sci. 95 (9) (1981) 2333–2335.
[9] J.H. She, K. Ueno, Effect of additive content on liquid-phase sintering on silicon carbide ceramics, Mater. Res. Bull. 34 (1999) 1629–1636.
[10] B.V. Manoj Kumar, M.H. Roh, Y.W. Kim, W. Kim, S.W. Park, W.S. Seo, Effect of additive composition on microstructure and mechanical properties of SiC ceramics sintered with small amount of RE_2O_3 (RE: Sc, Lu, Y) and AlN, J. Mater. Sci. 44 (2009) 5939–5943.
[11] V.A. Izhevskyi, A.H.A. Bressiani, J.C. Bressiani, Effect of liquid phase sintering on microstructure and mechanical properties of Yb_2O_3–AlN containing SiC-based ceramic, J. Am. Ceram. Soc. 88 (2005) 1115–1121.
[12] Y. Zhou, K. Hirao, M. Toriyama, Y. Yamauchi, S. Kanzaki, Effects of intergranular phase chemistry on the microstructure and mechanical properties of silicon carbide ceramics densified with rare-earth oxide and alumina additions, J. Am. Ceram. Soc. 84 (7) (2001) 1642–1644.
[13] R.M. German, Liquid Phase Sintering, Plenum Publication, New York, USA, 1985, 1 pp.

[14] R.M. German, P. Suri, S.J. Park, Review: liquid phase sintering, J. Mater. Sci. 44 (2009) 1–39.
[15] V.R.M. German, Sintering Theory and Practice, John Wiley and Sons, Inc., New York, NY, 1996.
[16] S. Prochazka, Ceramics for high-performance applications, in: Proceedings of the 2nd Army Materials Technology Conference, Hyannis, MS, 1973, pp. 239–252.
[17] T.S. Srivatsan, B.G. Ravi, M. Petraroli, T.S. Sudarshan, The microhardness and microstructural characteristics of bulk molybdenum samples obtained by consolidating nanopowders by plasma pressure compaction, Int. J. Refract. Met. Hard. Mater. 20 (2002) 181–186.
[18] M. Bothara, S.V. Atre, T. Sudarshan, R. Radhakrishnan, S.J. Park, R.M. German, Sintering behavior of nanocrystalline silicon carbide using a plasma pressure compaction system: master sintering curve analysis, Metall. Mater. Trans. A 41 (2010) 3252–3261.
[19] H.Y. Jin, M. Ishiyama, G.J. Qiao, J.Q. Gao, Z.H. Jin, Plasma active sintering of silicon carbide, Mater. Sci. Eng. A 483–484 (2008) 270–273.
[20] M.C. Rodriguez, A. Munoz, A.D. Rodriguez, Effect of atmosphere and sintering time on the microstructure and mechanical properties at high temperatures of α-SiC sintered with liquid phase Y_2O_3–Al_2O_3, J. Eur. Ceram. Soc. 26 (2006) 2397–2405.
[21] V.P. Onbattuvelli, S.V. Atre, Review of net shape fabrication of thermally conducting ceramics, Mater. Manuf. Process. 26 (6) (2011) 832–845.
[22] V.P. Onbattuvelli, S. Vallury, S. Laddha, S. Atre, Properties of SiC and AlN feedstocks for the powder injection moulding of thermal management devices, PIM Int. 4 (3) (2010) 64–70.
[23] V. Onbattuvelli, G. Purdy, G. Kim, S. Laddha, S. Atre, Powder injection molding of bimodal μ–n silicon carbide and aluminum nitride ceramics, Adv. Powder Metall. Part. Mater. 1 (2010) 64–72.
[24] V. Onbattuvelli. The effects of nano particle addition on the processing, structure and properties of SiC and AlN, Ph.D thesis, Oregon state University, Corvallis, (2010).
[25] M. Balog, K. Sedlackova, P. Zifcak, J. Janega, Liquid phase sintering of SiC with rare-earth oxides, Ceram. Silik 49 (2005) 259–262.
[26] J. Gao, H. Xiao, H. Du, Sol–gel synthesis and pressureless sintering of nanophase silicon carbide, J. Mater. Sci. Lett. 21 (2002) 1835–1837.
[27] O.B. Lopez, A.L. Ortiz, F. Guiberteau, Effect of microstructure on sliding-wear properties of liquid-phase-sintered α-SiC, J. Am. Ceram. Soc. 88 (8) (2005) 2159–2163.
[28] M. Herrmann, R. Neher, K. Brandt, S. Hoehn, Micro-segregations in liquid phase sintered silicon carbide ceramics, J. Eur. Ceram. Soc. 30 (2010) 1495–1501.
[29] M. Bothara, Sintering of Nanocrystalline Silicon Carbide in Plasma Pressure Compaction System, PhD Thesis, Oregon State University, USA, 2007.
[30] M. Nader, F. Aldinger, M.J. Hoffmann, Influence of the α/β-SiC phase transformation on microstructural development and mechanical properties of liquid phase sintered silicon carbide, J. Mater. Sci. 34 (1999) 1197–1204.
[31] G. Rixecker, K. Biswas, I. Wiedmann, F. Aldinger, J. Ceram. Process. Res. Vol. 1 (2009) 12–19.
[32] Y.W. Kim, J.Y. Kim, S.H. Rhee, D.Y. Kim, Effect of initial particle size on microstructure of liquid-phase sintered α-silicon carbide, J. Eur. Ceram. Soc. 20 (2000) 945–949.
[33] S.G. Lee, W.H. Shim, J.Y. Kim, Y.W. Kim, W.T. Kwon, Effect of sintering-additive composition on fracture toughness of liquid-phase-sintered SiC ceramics, J. Mater. Sci. Lett. 20 (2001) 143–146.
[34] Can, M. Herrmann, D.S. McLachlan, I. Sigalas, J. Adler, Densification of liquid phase sintered silicon carbide, J. Eur. Ceram. Soc. 26 (2006) 1707–1712.
[35] X.Z. Guo, H. Yang, Sintering and microstructure of silicon carbide with $Y_3Al_5O_{12}$ added by sol–gel method, J. Zhejiang Univers. Sci. 6B (3) (2005) 213–218.
[36] X. He, Y. Guo, Z. Yu, Y. Zhou, D. Jia, Study on microstructures and mechanical properties of short-carbon-fiber-reinforced SiC composites prepared by hot-pressing, Mater. Sci. Eng., A 527 (2009) 334–338.
[37] V.V. Pujar, R.P. Jensen, N.P. Padture, Densification of liquid-phase-sintered silicon carbide, J. Mater. Sci. Lett. 19 (2000) 1011–1014.
[38] G. Magnani, L. Beaulardi, L. Pilotti, Properties of liquid phase pressure-less sintered silicon carbide obtained without sintering bed, J. Eur. Ceram. Soc. 25 (2005) 1619–1627.
[39] K. Suzuki, M. Sasaki, Effects of sintering atmosphere on grain morphology of liquid-phase-sintered SiC with Al_2O_3 additions, J. Eur. Ceram. Soc. 25 (2005) 1611–1618.
[40] Y. Zhang, J. Han, L. Hu, The effect of sintering additive on fracture behavior of carbon–whisker–reinforced silicon carbide composites, Mater. Sci. Eng., A 480 (2008) 62–67.
[41] F.J. Clemens, V. Wallquist, W. Buchser, M. Wegmann, T. Graule, Silicon carbide fiber-shaped microtools by extrusion and sintering SiC with and without carbon powder sintering additive, Ceram. Int. 33 (2007) 491–496.